J Comput Electron (2015) 14:43–50
DOI 10.1007/s10825-014-0627-3

A Deterministic approach to noise in a non-equilibrium electron–phonon system based on the Boltzmann equation

Mindaugas Ramonas · Christoph Jungemann

Published online: 26 September 2014

Abstract A deterministic model for electron velocity fluctuations in a non-equilibrium bulk electron–phonon system is presented. The model is based on the spherical harmonics expansion of the system of the two coupled Boltzmann equations for electrons and phonons. Bulk GaN at 300 K ambient temperature is selected as a model system. The Langevin approach is used for noise calculations, and expressions for the power spectral density of the electron velocity fluctuations are presented in the paper. Convergence behavior of the model is discussed in detail. Results of the developed noise model are verified against a consistent Monte Carlo model, and excellent agreement is obtained in the range of frequencies, where the Monte Carlo method yields reliable results. Introduction of nonequilibrium phonons substantially increases the electron noise temperature at frequencies below 100 GHz.

Keywords Langevin-Boltzmann equation · Hot electrons · Hot phonons · Electron velocity fluctuations

1 Introduction

Non-equilibrium distributions of carriers are relatively easy induced in the channels of the modern nanoscale devices [1]. In polar semiconductors the main path of energy dissipation for electrons is longitudinal optical (LO) phonon emission. The power supplied by the electric field is shared between the coupled nonequilibrium (hot) electron and phonon subsystems. The impact of hot phonons on steady state electron transport under strong external electrical fields is discussed in [2,3]. The buildup of hot phonons (hot phonon effect) forms the bottleneck for the electron energy dissipation [4]. Recently the impact of hot phonons on the high frequency performance of GaN-based HEMT and degradation of power devices was investigated using the fluctuation technique [5].

Electron velocity fluctuations are an important source of information about physical processes taking part in the semiconductor [6]. The Monte Carlo (MC) method is usually used to investigate noise properties of semi-classical Boltzmann systems [7,8]. Due to its stochastic nature, the MC method allows direct evaluation of the correlation functions in the time domain. In case of system with different time scales (e.g. in bulk GaN the LO-phonon emission time is in the femtosecond range, whereas the hot LO-phonon lifetime is in the picosecond range), an excessive amount of computational time is required to obtain correlation functions with the required accuracy. Alternatives to the MC method are deterministic methods, dealing with the Boltzmann equation in the frequency domain.

Spherical harmonics [9] and multigroup [10] approaches were applied for investigation of electron DC transport in bulk non-equilibrium electron–phonon systems. In the present paper, to the authors knowledge for the first time, a deterministic model for electron velocity fluctuations in a non-equilibrium bulk electron–phonon system in the frequency domain is presented. The model is based on the spherical harmonics expansion of system of the two Boltzmann equations for electrons and phonons [9]. The Langevin method is used for the calculation of the power spectral density (PSD) of the electron velocity fluctuations [11]. The Langevin method involves the Green's functions and gives

M. Ramonas (✉) · C. Jungemann
Chair of Electromagnetic Theory, RWTH Aachen University, 52056 Aachen, Germany
e-mail: ramonas@pfi.lt

M. Ramonas
Fluctuation Research Laboratory, Semiconductor Physics Institute, Center for Physical Sciences and Technology, A. Goštauto str. 11, 01108 Vilnius, Lithuania

more information on physical processes in the system than the MC method.

2 Theory

In the semi-classical approach the evolution of the non-equilibrium electron–phonon system in time is described by two coupled nonlinear Boltzmann equations for the distribution functions of the electrons $f(\mathbf{k}, t)$ and LO phonons $n(\mathbf{q}, t)$ in the 6-dimensional space of electron and phonon momenta $\{\mathbf{k}, \mathbf{q}\}$. If the Pauli exclusion principle and electron-electron interaction are neglected and a homogeneous bulk system is assumed, the kinetic equation for the electron distribution function takes the form:

$$\frac{\partial f(\mathbf{k}, t)}{\partial t} - \frac{e}{\hbar}\mathbf{E}\nabla_k f(\mathbf{k}, t) + \mathrm{I}_k[f] + \Pi_k^{(\mathrm{LO})}[f, n] = 0, \quad (1)$$

where e is the positive electron charge, $\hbar$ Planck's constant divided by 2π, and $\mathbf{E}$ the applied electric field. A magnetic field is neglected and the electron distribution function is defined for a single spin state assuming spin degeneracy. The scattering rate

$$\mathrm{I}_k[f](\mathbf{k}, t) = \frac{V_0}{(2\pi)^3}\sum_i \int \left\{W_i(\mathbf{k}, \mathbf{k}')f(\mathbf{k}, t) - W_i(\mathbf{k}', \mathbf{k})f(\mathbf{k}', t)\right\} d^3k' \quad (2)$$

represents the linear part of the scattering integral (electron interaction with ionized impurities and intra-valley acoustic phonons, for which the Bose-Einstein distribution with the lattice temperature is assumed). $W_i(\mathbf{k}, \mathbf{k}')$ is the transition rate of the ith scattering process and V_0 the volume of the bulk system. The integral runs over all final states. These scattering processes are described in detail in the literature (e.g. [12]).

The nonlinear operator $\Pi_k^{(\mathrm{LO})}[]$ defines the electron interaction with the non-equilibrium LO phonons. It is based on the transition rate of the electron–LO-phonon interaction [13]. For absorption we obtain:

$$W_{\mathrm{abs}}[n](\mathbf{q}, \mathbf{k}, \mathbf{k}', t) = \frac{\pi\omega_0 e^2}{q^2 V_0}\left[\frac{1}{\varepsilon_\infty} - \frac{1}{\varepsilon_0}\right] n(\mathbf{q}, t) \delta(\mathbf{k}' - [\mathbf{k} + \mathbf{q}])\delta(\epsilon(\mathbf{k}') - [\epsilon(\mathbf{k}) + \hbar\omega_0]), \quad (3)$$

where ε_0 and ε_∞ are the static and high frequency permittivities of the investigated material. $\hbar\omega_0$ is the energy of the LO phonon, which is assumed to be dispersionless, and $\epsilon(\mathbf{k})$ the conduction band energy. The electron is scattered from the initial state $\mathbf{k}$ into the final one $\mathbf{k}'$ for a given phonon momentum $\mathbf{q}$. For emission the spontaneous emission has to be taken into account in addition to the stimulated one:

$$W_{\mathrm{em}}[n](\mathbf{q}, \mathbf{k}, \mathbf{k}', t) = \frac{\pi\omega_0 e^2}{q^2 V_0}\left[\frac{1}{\varepsilon_\infty} - \frac{1}{\varepsilon_0}\right] [n(\mathbf{q}, t) + 1] \delta(\mathbf{k}' - [\mathbf{k} - \mathbf{q}])\delta(\epsilon(\mathbf{k}') - [\epsilon(\mathbf{k}) - \hbar\omega_0]), \quad (4)$$

and the sign of the phonon energy and momentum changes in the delta functions compared to the case of absorption. With the transition rates the operator for scattering of electrons with LO phonons takes the form:

$$\Pi_k^{(\mathrm{LO})}[f, n](\mathbf{k}, t) = \frac{V_0}{(2\pi)^3}\sum_\nu \int\int \{W_\nu[n](\mathbf{q}, \mathbf{k}, \mathbf{k}', t)f(\mathbf{k}, t) - W_\nu[n](\mathbf{q}, \mathbf{k}', \mathbf{k}, t)f(\mathbf{k}', t))\} d^3k' d^3q. \quad (5)$$

The sum runs over absorption and emission. The first term in the integral describes the scattering out of the state $\mathbf{k}$ and the second one into it. The scattering integral is nonlinear due to the product of the electron and phonon distributions.

LO-phonon absorption and stimulated emission is proportional to the LO-phonon distribution function, which in general deviates from the equilibrium one defined by the Bose-Einstein statistics. The kinetic equation for the LO-phonon distribution function is given by:

$$\frac{\partial n(\mathbf{q}, t)}{\partial t} + \mathrm{I}_q^{(\mathrm{th})}[n] + \Pi_q^{(\mathrm{el})}[n, f] = 0, \quad (6)$$

where the drift term is absent because of the usual assumption of dispersionless LO phonons. The linear operator $\mathrm{I}_q^{(\mathrm{th})}[]$ represents the decay of the non-equilibrium LO phonons into other modes of crystal lattice vibrations (acoustic phonons and electrically inactive optical phonons). This operator is usually formulated in the relaxation time approximation [3]:

$$\Pi_q^{(\mathrm{th})}[n](\mathbf{q}, t) = \frac{n(\mathbf{q}, t) - n_{\mathrm{eq}}}{\tau_{\mathrm{ph}}}. \quad (7)$$

Here n_{eq} stands for the equilibrium Bose-Einstein distribution for the lattice temperature (temperature of the thermal bath), and τ_{ph} is the LO-phonon life time.

By each electron–LO-phonon scattering event an LO phonon is either created (phonon emission) or annihilated (phonon absorption) and the net LO-phonon annihilation rate in Eq. (6) is given by:

$$\Pi_q^{(\mathrm{el})}[n, f](\mathbf{q}, t) = \frac{2V_0}{(2\pi)^3}\int\int \{W_{\mathrm{abs}}[n](\mathbf{q}, \mathbf{k}, \mathbf{k}', t) - W_{\mathrm{em}}[n](\mathbf{q}, \mathbf{k}, \mathbf{k}', t)\} f(\mathbf{k}, t) d^3k' d^3k. \quad (8)$$

The second integral runs over all initial electron states $\mathbf{k}$ in contrast to Eq. (5), where it runs over all phonon momenta $\mathbf{q}$. The factor of 2 is due to spin degeneracy in the electron

system. Both Boltzmann equations (1) and (6) are nonlinearly coupled due to the product of the electron and phonon distribution functions in Eqs. (5) and (8).

Noise is calculated by the Langevin approach [11]. To this end the coupled Boltzmann equations (1) and (6) are linearized in the electron and phonon distribution functions:

$$L_\mathrm{e}[n,\, f](\mathbf{k}, t) = 0 \tag{9}$$

$$L_\mathrm{ph}[n,\, f](\mathbf{q}, t) = 0 \tag{10}$$

where $L_\mathrm{e}[]$ is the linear operator for Eq. (1) and $L_\mathrm{ph}[]$ for Eq. (6). The linearized Boltzmann equations are solved for sources, which describe either the generation of a single electron:

$$L_\mathrm{e}[G^\mathrm{e}_\mathrm{ph},\, G^\mathrm{e}_\mathrm{e}](\mathbf{k}, t) = \frac{(2\pi)^3}{V_0}\delta(\mathbf{k}-\mathbf{k}')\delta(t-t') \tag{11}$$

$$L_\mathrm{ph}[G^\mathrm{e}_\mathrm{ph},\, G^\mathrm{e}_\mathrm{e}](\mathbf{q}, t) = 0 \tag{12}$$

or LO phonon:

$$L_\mathrm{e}[G^\mathrm{ph}_\mathrm{ph},\, G^\mathrm{ph}_\mathrm{e}](\mathbf{k}, t) = 0 \tag{13}$$

$$L_\mathrm{ph}[G^\mathrm{ph}_\mathrm{ph},\, G^\mathrm{ph}_\mathrm{e}](\mathbf{q}, t) = \frac{(2\pi)^3}{V_0}\delta(\mathbf{q}-\mathbf{q}')\delta(t-t'). \tag{14}$$

Care has to be taken in the formulation of the linear system to avoid double counting due to, for example, spin degeneracy [14]. Two sets of Green's functions are obtained. $G^\mathrm{e}_\mathrm{e}(\mathbf{k}, t; \mathbf{k}', t')$ is the response of the electron system in state $\mathbf{k}$ at time t to the generation of an electron in state $\mathbf{k}'$ at time t' and $G^\mathrm{e}_\mathrm{ph}(\mathbf{q}, t; \mathbf{k}', t')$ the corresponding response of the phonon system. In the case of the generation of a phonon we get $G^\mathrm{ph}_\mathrm{e}(\mathbf{k}, t; \mathbf{q}', t')$ and $G^\mathrm{ph}_\mathrm{ph}(\mathbf{q}, t; \mathbf{q}', t')$. Since we are interested only in velocity fluctuations of electrons in a stationary system, we can define simpler Green's functions for those fluctuations:

$$G^\mathrm{e}_v(t-t', \mathbf{k}') = \frac{V_0}{(2\pi)^3}\int \mathbf{v}(\mathbf{k}) G^\mathrm{e}_\mathrm{e}(\mathbf{k}, t-t'; \mathbf{k}', 0) d^3k \tag{15}$$

$$G^\mathrm{ph}_v(t-t', \mathbf{q}') = \frac{V_0}{(2\pi)^3}\int \mathbf{v}(\mathbf{k}) G^\mathrm{ph}_\mathrm{e}(\mathbf{k}, t-t'; \mathbf{q}', 0) d^3k. \tag{16}$$

Fourier transformation with respect to $t-t'$ yields the transfer functions:

$$G^\mathrm{e}_v(\mathbf{k}, \omega) = \int_0^\infty G^\mathrm{e}_v(t, \mathbf{k}) \exp(-i\omega t) dt \tag{17}$$

$$G^\mathrm{ph}_v(\mathbf{q}, \omega) = \int_0^\infty G^\mathrm{e}_v(t, \mathbf{q}) \exp(-i\omega t) dt, \tag{18}$$

where ω is the angular frequency.

There are three sources of noise: the linear scattering operator of the electron Boltzmann equation, electron–LO-Phonon scattering and the relaxation term of the phonon Boltzmann equation. They all describe instantaneous scattering and the corresponding PSDs are white.

The linear scattering operator describes the transition of an electron from state $\mathbf{k}$ into state $\mathbf{k}'$. This can be viewed as annihilation of an electron in state $\mathbf{k}$ and creation of a new electron in state $\mathbf{k}'$, and the combined transfer function for the scattering event is given by $G^\mathrm{e}_v(\mathbf{k}', \omega) - G^\mathrm{e}_v(\mathbf{k}, \omega)$. The scattering process itself is a Poisson process of which the white PSD is given by twice the transition probability rate $2\sum_i W_i(\mathbf{k}, \mathbf{k}') f_0(\mathbf{k})$, where $f_0(\mathbf{k})$ is the stationary distribution function of the electrons [11,15]. The corresponding PSD for the velocity fluctuations can be obtained with the Wiener-Lee theorem [16] and integration over all initial and final states

$$S^\mathrm{e}_{vv}(\omega) = \frac{4V_0^2}{N_0(2\pi)^6}\sum_i \int\int W_i(\mathbf{k}, \mathbf{k}') f_0(\mathbf{k}) \\ |G^\mathrm{e}_v(\mathbf{k}', \omega) - G^\mathrm{e}_v(\mathbf{k}, \omega)|^2 d^3k' d^3k. \tag{19}$$

The factor of four is due to spin degeneracy and the use of two-sided PSDs. The PSD is normalized to a single electron and the number of electrons in the stationary state is calculated by

$$N_0 = \frac{2V_0}{(2\pi)^3}\int f_0(\mathbf{k}) d^3k. \tag{20}$$

Scattering of an electron with an LO phonon yields

$$S^\text{e-ph}_{vv}(\omega) = \frac{4V_0^2}{N_0(2\pi)^6}\sum_\nu \int\int\int W_\nu[n_0](\mathbf{q}, \mathbf{k}, \mathbf{k}') f_0(\mathbf{k}) \\ |G^\mathrm{e}_v(\mathbf{k}', \omega) - G^\mathrm{e}_v(\mathbf{k}, \omega) \mp G^\mathrm{ph}_v(\mathbf{q}, \omega)|^2 d^3k' d^3k d^3q. \tag{21}$$

$n_0(\mathbf{q})$ is the stationary distribution function of LO phonons. The upper sign is to be used for absorption (annihilation of a phonon) and the lower one for emission (creation). Eq. (21) is the straightforward generalization of Eq. (19). An electron is scattered from state $\mathbf{k}$ into the state $\mathbf{k}'$ and in the case of absorption an LO phonon is annihilated and the combined transfer function is given by $G^\mathrm{e}_v(\mathbf{k}', \omega) - G^\mathrm{e}_v(\mathbf{k}, \omega) - G^\mathrm{ph}_v(\mathbf{q}, \omega)$. In the case of emission creation is considered by a plus sign.

The LO-phonon relaxation term involves only creation and annihilation of LO phonons and the corresponding PSD is rather simple

$$S^\mathrm{ph}_{vv}(\omega) = \frac{2V_0}{N_0(2\pi)^3}\int \frac{n_0(\mathbf{q}) + n_\mathrm{eq}}{\tau_\mathrm{ph}} |G^\mathrm{ph}_v(\mathbf{q}, \omega)|^2 d^3q, \tag{22}$$

and can be calculated in the same way as noise due to generation/recombination [17]. The contributions of the involved

non-polar phonons are neglected and the factor of two accounts for the two-sided PSD. The total PSD is given by the sum of the three contributions.

The above equations are solved by numerical means. The electron distribution function is expanded over the momentum space with respect to the angles of spherical coordinates by spherical harmonics of arbitrary order [18,19]. The absolute value of the momentum is converted to energy, which is discretized on an equidistant grid. The phonon distribution function is treated similarly with the exception that instead of the energy the modulus of the phonon momentum is used. Care is taken to ensure that the discrete Boltzmann equations are particle number conserving. The resultant system of nonlinear equations is solved with the Newton-Raphson method. The transfer functions (17) and (18) are CPU efficiently calculated by the adjoint method [20].

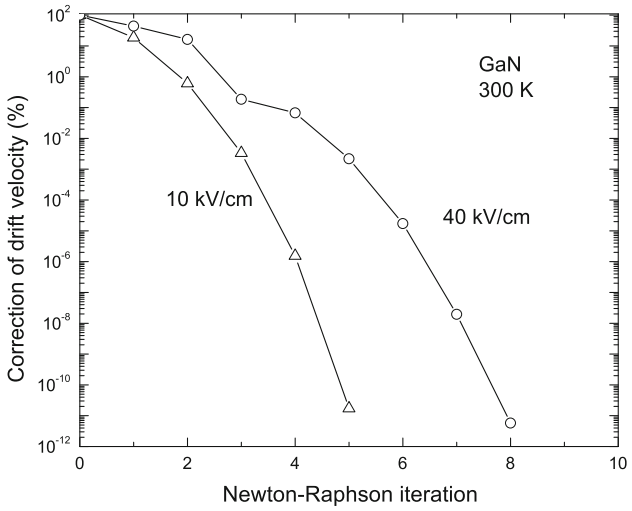

Fig. 1 Convergence behavior of the Newton-Raphson solver for the electron/phonon system for two values of the applied electric field: *open triangles* 10 kV/cm and *open circles* 40 kV/cm

3 Results

Due to the strong electron–LO-phonon interaction, bulk wurtzite GaN at 300 K ambient temperature is selected to verify the Langevin-Boltzmann equation based approach for noise calculation. For wurtzite-phase GaN, the conduction band minimum is located at the Γ point. In the range of the investigated electric fields, electron transfer into higher valleys of the conduction band is expected to be negligible. In our model electron transport perpendicular to the c axis of the crystal is simulated, where the simple transverse effective mass approximation for a single parabolic valley is applicable.

In the present manuscript we concentrate on electron interaction with lattice vibrations, and only the electron interaction with acoustic and LO phonons is taken into account. Electron scattering by acoustic phonons at room temperature is usually treated as an elastic process because the energies of the involved acoustic phonons are small. This approach restricts the investigation of electron transport in GaN to electric fields higher than 2 kV/cm (due to the high LO phonon energy, acoustic phonons take a substantial part in electron energy dissipation close to equilibrium). The acoustic phonons are assumed to remain in equilibrium because the remote heat sink can be easily reached by the excess acoustic phonons. Acoustic phonon scattering via deformation potential is considered, where the deformation potential is treated as a scalar quantity.

The polar LO-phonon scattering is taken into account in the cubic approximation. Unlike acoustic modes, the excess LO phonons remain where they are generated. To avoid electron gas degeneracy the electron gas density is set to 10^{18}cm^{-3}, for which the electron state occupancy is well below one. The LO-phonon relaxation time is decided by the vibrational properties of the investigated material. For bulk GaN at room temperature, the experimental values of the LO phonon relaxation time are in the range of 2.5–0.35 ps, depending on the electron gas density [21]. In our calculations an LO-phonon relaxation time of 1 ps is used. The electron effective mass, and scattering parameters are the same as in Ref. [22].

First of all, convergence properties of the solver for the modeled electron-phonon system have to be discussed. In the Newton-Raphson method the Jacobian matrix for the full system of coupled nonlinear equations is constructed and used to calculate the corrections to the initial guess for the electron and phonon distribution functions until convergence is achieved.

The Newton-Raphson loop starts from the equilibrium electron and phonon distribution functions, and in Fig. 1 typical convergence behavior of the simulation is shown for two values of the applied electric field: 10 and 40 kV/cm. Eight spherical harmonics are used for the electron distribution function and four spherical harmonics for the phonon distribution function. For both electrical fields fast quadratic convergence is obtained. At 10 kV/cm (open triangles) five Newton-Raphson iterations are enough to calculate the electron drift velocity within the numerical accuracy. At 40 kV/cm (open squares) displacement of the electron-phonon system from equilibrium is stronger and the same accuracy is obtained after eight iterations.

To formulate the system of coupled kinetic equations (1) and (6) in spherical harmonics, both the electron and LO-phonon distribution functions are expressed by an infinite spherical harmonics expansions. To obtain a numerically manageable system of equations, both expansions for the electron and phonon distributions are truncated.

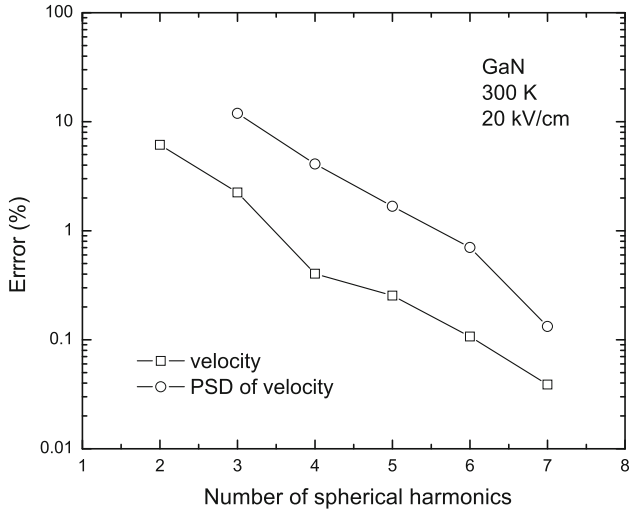

Fig. 2 Error of the electron drift velocity (*open squares*) and PSD of velocity fluctuations at 1 GHz frequency (*open circles*) for different numbers of spherical harmonics for the electron distribution function. The *error* is evaluated relative to the values where eight spherical harmonics for electrons are included

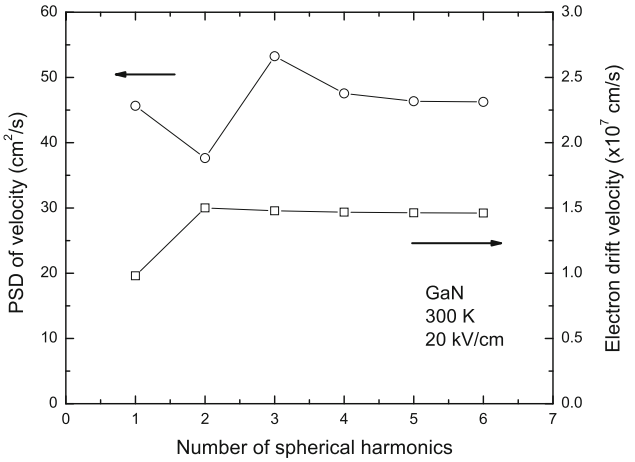

Fig. 3 The dependence of the electron drift velocity (*open squares*) and PSD of the velocity fluctuations (*open circles*) at 1 GHz frequency on the number of spherical harmonics used for the expansion of the phonon distribution function

Figure 2 shows the error of the electron drift velocity and PSD of velocity fluctuations at 1 GHz frequency for different numbers of spherical harmonics for the electron distribution function. The error is evaluated relative to the values where eight spherical harmonics for electrons are included. Four spherical harmonics are used in the expansion of the phonon distribution function.

At least four spherical harmonics for the electron distribution function are required to obtain an error of the electron drift velocity below 1 %. The PSD of the velocity fluctuations is more sensitive to the number of the spherical harmonics for the electron distribution function, and six or more spherical harmonics are necessary to obtain an error below 1 %. To reach sufficient accuracy in the whole range of the applied electric field, in our calculations eight spherical harmonics are included for the electron distribution function.

The dependence of the electron drift velocity and PSD of the velocity fluctuations at 1 GHz frequency and 20 kV/cm applied electric field on the number of spherical harmonics used for the expansion of the phonon distribution function is presented in Fig. 3. If only one spherical harmonic is used in the simulator, an angular independent phonon distribution function is assumed. Due to applied electric field, and anisotropic nature of polar LO-phonon scattering rate, the LO-phonon distribution is anisotropic. To account for the angular dependence of the phonon distribution function, at least two spherical harmonics are necessary. Due to the phonon drag, the introduction of the second spherical harmonic increases the electron drift velocity (open squares in Fig. 3). The PSD of the velocity fluctuations is again more sensitive to the number of the spherical harmonics as the mean electron velocity (cf. open squares and circles in Fig. 3), and four spherical harmonics are used for the phonon distribution function to obtain sufficient accuracy for the noise calculations.

The correctness of the calculated Green's functions and validity of the expressions for the PSD of velocity fluctuations (19), (21) and (22) are verified by the comparison of the deterministic approach with the MC model. The semiclassical ensemble MC algorithm is employed, and the band structure, scattering mechanisms and material parameters are the same as in the spherical harmonics model.

In the MC algorithm each LO-phonon generation or annihilation event due to their interaction with the electrons is registered in a histogram. The resultant histogram is used to calculate the time-dependent phonon distribution. To obtain the steady state, the nonequilibrium LO-phonon interaction with the thermal bath is included in the hot-phonon relaxation time approximation. In order to correctly account for the velocity fluctuations due to random LO-phonon relaxation (Eq. (22)), after each MC time step the LO-phonon distribution function is updated by the random creation or annihilation of LO phonons according to the corresponding probability.

The algorithm subdivides the total simulation time into equal time intervals, and the time-dependent ensemble averages for the quantities of interest are calculated. The collected data on the time-dependent electron drift velocity are used to calculate the electron drift velocity autocorrelation function. Fourier transform of the autocorrelation function yields the corresponding PSD.

In Fig. 4 the PSD of the electron drift velocity fluctuations calculated using the spherical harmonics based Langevin approach are compared with MC results. Excellent

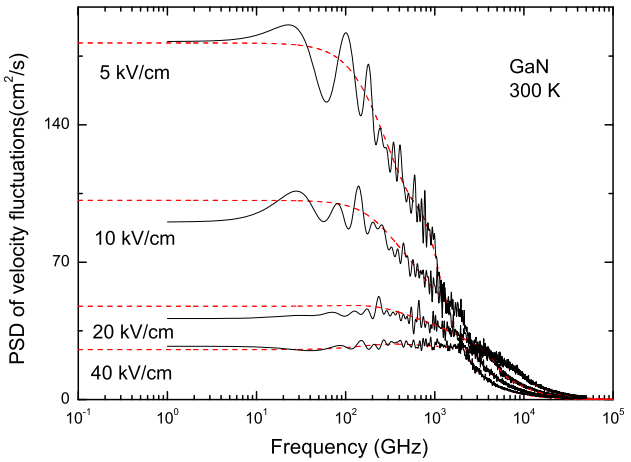

Fig. 4 The PSD of the electron drift velocity fluctuations calculated using the spherical harmonics based Langevin approach (*dashed lines*) and the MC method (*noisy solid lines*)

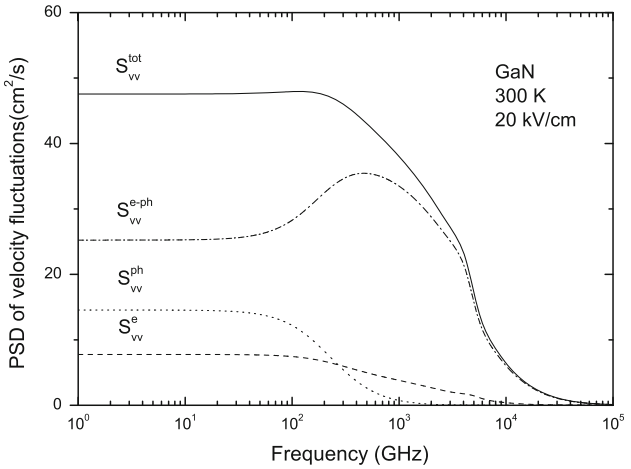

Fig. 5 Constituents of the PSD of the electron drift velocity fluctuations. The PSD due to acoustic phonon *scattering–dashed line*, PSD due to LO-phonon scattering in electron kinetic equation–*dash-dotted line*, PSD due to LO-phonon relaxation in phonon kinetic equation–*dotted line*. The sum of all constituents is given by the *solid line*

agreement is obtained between the Langevin and MC approaches at four different applied electric fields: 5, 10, 20 and 40 kV/cm above the 100 GHz frequency (cf. Fig. 4 dashed and solid lines). At lower frequencies due to the stochastic nature of the MC method the accuracy of the MC results is questionable. In contrary, the spherical harmonics approach allows the calculation of the PSD down to zero frequency.

The PSD of the electron drift velocity fluctuations calculated by the Langevin approach (solid line in Fig. 5) can be splitted into separate parts to investigate the influence of the different scattering mechanisms. The dashed line in Fig. 5 represents the PSD of the electron drift velocity fluctuations due to acoustic phonon scattering $S^{\mathrm{e}}_{\mathrm{vv}}$ (Eq. (19)). The bigger part of the PSD, however comes from the nonequilibrium

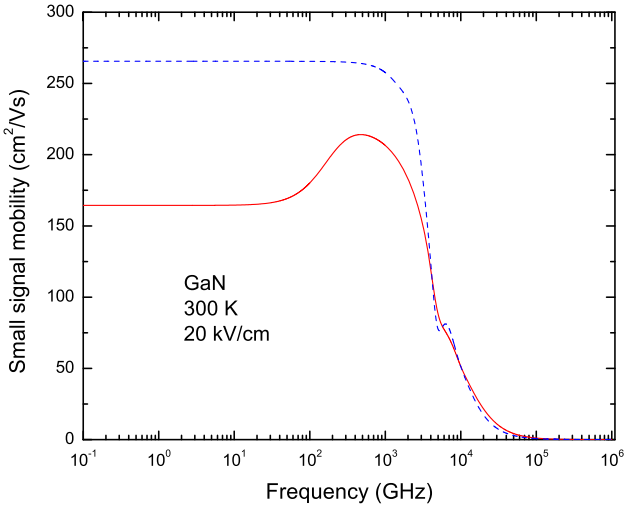

Fig. 6 Spectra of the electron small signal mobility with (*solid line*) and without (*dashed line*) hot phonons for 20 kV/cm

LO-phonon scattering $S^{\mathrm{e-ph}}_{\mathrm{vv}}+S^{\mathrm{ph}}_{\mathrm{vv}}$ (Eqs. (21) and (22)) (doted and dash-doted lines in Fig. 5)). The onset of the PSD due to LO-phonon relaxation term in the phonon kinetic equation $S^{\mathrm{ph}}_{\mathrm{vv}}$ is defined by the inverse of the LO-phonon life time (doted line in Fig. 5). The PSD due to the LO-phonon relaxation is significant, and has to be included for the analysis of the noise below the frequency decided by the LO-phonon life time.

Transfer functions contain information on the small signal behavior of the investigated electron-phonon system. The velocity transfer functions (17) and (18) necessary for the calculation of the PSD of the electron drift velocity fluctuations, can be employed in the calculation of the response of the electron drift velocity to a small variation in the applied external electric field. Figure 6 shows spectra of the electron small signal mobility with and without the hot phonons for 20 kV/cm. At high frequencies the influence of hot phonons is small. However, in the range of frequencies important for high speed device operation (below 100 GHz), due to hot-phonon–induced additional friction, the small signal mobility is significantly reduced (cf. solid and dashed line in Fig. 6).

The equivalent electron noise temperature is often measured in experiments on hot-electron noise in bulk semiconductors. In case of a constant electron density the noise temperature in the direction of the applied electric field is defined as [6]:

$$T_n(E,\omega)=\frac{eS_{vv}(E,\omega)}{4k_{\mathrm{B}}\mathrm{Re}\{\mu(\mathrm{E},\omega)\}}, \tag{23}$$

here $\mu(E,\omega)$ is the electron small signal mobility. Both, the PSD of the electron velocity fluctuations and the small signal mobility calculated by means of MC simulations contain

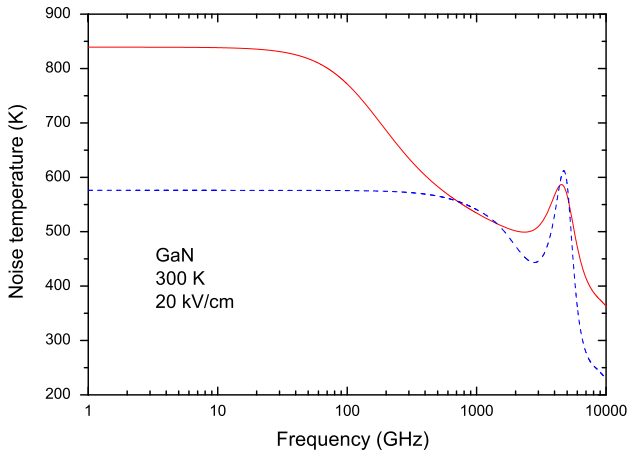

Fig. 7 Spectra of the electron noise temperature with (*solid line*) and without (*dashed line*) hot phonons for 20 kV/cm

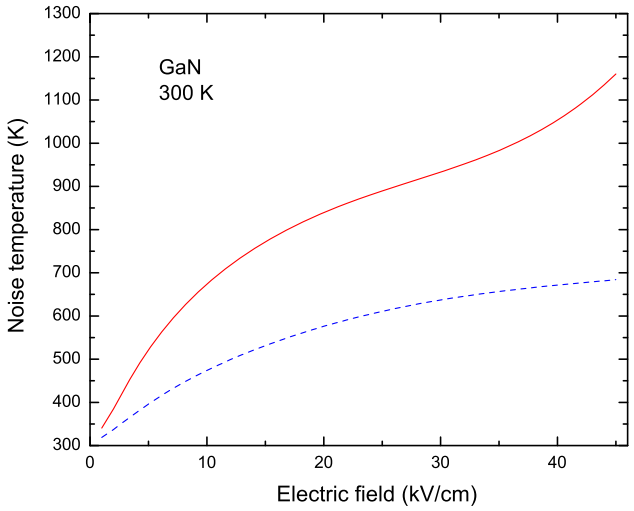

Fig. 8 The dependence of the calculated electron noise temperature at 1 GHz frequency on the applied electric field with (*solid line*) and without (*dashed line*) hot phonons at a lattice temperature of 300 K

stochastic errors, making the evaluation of the electron noise temperature difficult.

In the Langevin approach the same transfer functions are used to calculate the PSD of the electron velocity fluctuations and the small signal mobility, thus no additional effort is required to evaluate the electron noise temperature. Figure 7 shows the spectra of the electron noise temperature with and without the hot phonons for 20 kV/cm. Due to the hot phonons the electron noise temperature substantially increases at frequencies below 100 GHz.

In the range of the electric field, where the main energy loss is due to LO-phonon emission, a resonant hot-electron noise behavior is observed. The resonance is caused by the streaming motion of electrons, terminated by the LO-phonon emission. The frequency of the resonance is defined by the time required for an electron with zero initial energy to reach the LO-phonon energy [6]:

$$\tau_{\mathrm{r}} = \frac{\sqrt{2m_{\mathrm{el}}\hbar\omega_0}}{eE}, \tag{24}$$

where m_{el} is the electron effective mass. The peak of the resonance is obtained at 4,500 GHz frequency (Fig. 7, dashed line), in reasonable agreement with Eq. 24. If hot phonons are included, the frequency of the resonance remains the same, however due to the increase in electron-LO phonon interaction, the strength of the resonance is reduced (Fig. 7, solid line).

In Fig. 8 the dependence of the calculated electron noise temperature on applied electric field is presented without hot phonons (dashed line) and with hot phonons (solid line). According to the Nyquist theorem, at zero electric field the electron noise temperature reaches the ambient temperature. Calculated values of the noise temperature both with and without hot phonons at low electric field approach the lattice temperature (Fig. 8, solid and dashed lines).

If acoustic phonon scattering in the elastic approximation is used, it is not possible to obtain the stationary solution of the kinetic equations (1) and (6) near equilibrium. To verify our calculations against the Nyquist theorem, at zero electric field equilibrium distributions are used for the stationary distributions of electrons and phonons in the linearized equations for the Green's function calculation and excellent agreement with the Nyquist theorem is obtained.

An external electric field heats the coupled electron-phonon system; the energy of the chaotic motion of the electrons increases together with the noise temperature. Due to the reabsorption of the previously emitted LO phonons, hot phonons form the bottleneck for the electron energy dissipation, and noise temperature is increased with respect to the situation without hot phonons (cf. solid and dashed line in Fig. 8).

4 Conclusions

A deterministic approach based on the spherical harmonics expansion of the Boltzmann transport equation to calculate the power spectral density of the electron velocity fluctuations in a non-equilibrium electron-phonon system is presented. Expressions for the Langevin noise sources of the coupled electron-phonon system are given. The resultant system of nonlinear equations is solved with the Newton-Raphson method, and fast quadratic convergence is obtained. Eight spherical harmonics for the electron distribution function, and four spherical harmonics for the phonon distribution are enough to include all relevant phenomena for electric fields up to 45 kV/cm.

The correctness of the calculated Green's functions and validity of the expressions for the power spectral density of the velocity fluctuations are verified by comparison of the deterministic approach with the MC model; good agreement is obtain for electric fields up to 40 kV/cm. In strong electric fields and in the range of frequencies important for high speed device operation (below 100 GHz) due to hot-phonon–induced additional friction the small signal mobility is significantly reduced. Due to hot phonons the electron noise temperature substantially increases at frequencies below 100 GHz.

Acknowledgments Financial support by the "Deutsche Forschungsgemeinschaft" (DFG) is gratefully acknowledged. M. Ramonas is grateful for the partial funding by the European Social Fund under the Global Grant measure (Grant N VP1-3.1-ŠMM-07-K-03-038).

References

1. Shank, C., Zakharchenya, B.: Spectroscopy of Nonequilibrium Electrons and Phonons, Ser. Modern Problems in Condensed Matter Sciences. North-Holland, Amsterdam (1992)
2. Kocevar, P.: Hot phonon dynamics. Physica **134B**, 155–163 (1985)
3. Rieger, M., Kocevar, P., Lugli, P., Bordone, P., Reggiani, L., Goodnick, S.M.: Monte Carlo studies of nonequilibrium phonon effects in polar semiconductors and quantum wells. II. Non-Ohmic transport in n-type gallium arsenide. Phys. Rev. B **39**, 7866–7875 (1989)
4. Ramonas, M., Matulionis, A., Liberis, J., Eastman, L.F., Chen, X., Sun, Y.-J.: Hot-phonon effect on power dissipation in a biased AlGaN/AlN/GaN channel. Phys. Rev. B **71**, 075 324-1–075 324-8 (2005)
5. Matulionis, A.: Electron density window for best frequency performance, lowest phase noise and slowest degradation of GaN heterostructure field-effect transistors. Semicond. Sci. Technol. **28**(7), 074007 (2013)
6. Hartnagel, H., Katilius, R., Matulionis, A.: Microwave Noise in Semiconductor Devices. Wiley, New York (2001)
7. Starikov, E., Shiktorov, P., Gružinskis, V., Reggiani, L., Varani, L., Vaissiére, J.C., Palermo, C.: Monte Carlo calculations of hot-electron transport and diffusion noise in GaN and InN. Semicond. Sci. Technol. **20**(3), 279 (2005)
8. Bordone, P., Reggiani, L., Varani, L., Kuhn, T.: Hot-phonon effect on noise and diffusion in GaAs. Semicond. Sci. Technol. **9**(5S), 623 (1994)
9. Ramonas, M., Jungemann, C.: "Spherical harmonics solver for coupled hot-electron-hot-phonon system". In: 2013 International Conference on Simulation of Semiconductor Processes and Devices (SISPAD), pp. 360–363. Sep 2013
10. Galler, M., Schürrer, F.: Multigroup equations to the hot-electron hot-phonon system in III-V compound semiconductors. Comput. Methods Appl. Mech. Eng. **194**(2526), 2806–2818 (2005)
11. Kogan, S.: Electronic Noise and Fluctuations in Solids. Cambridge University Press, Cambridge (1996)
12. Jacoboni, C., Lugli, P.: The Monte Carlo Method for Semiconductor Device Simulation. Springer, Wien (1989)
13. Ridley, B.K.: Quantum Processes In Semiconductors, 2nd edn. Clarendon Press, Oxford (1988)
14. Jungemann, C.: "A deterministic solver for the Langevin Boltzmann equation including the Pauli principle". SPIE **6600**, 660 007-1–660 007-12 (2007)
15. Jungemann, C.: A deterministic approach to RF noise in silicon devices based on the Langevin Boltzmann equation. IEEE Trans. Electron Dev. **54**(5), 1185–1192 (2007)
16. Papoulis, A.: Probability, Random Variables, and Stochastic Processes, 4th edn. McGraw-Hill, New York (2001)
17. Bonani, F., Ghione, G.: Noise in Semiconductor Devices, Modeling and Simulation, ser. Advanced Microelectronics. Springer, Berlin (2001)
18. Hennacy, K.A., Goldsman, N.: A Generalized Legendre polynimial/sparse matrix approach for determining the distribution function in non-polar semiconductors. Solid-State Electron. **36**, 869–877 (1993)
19. Jungemann, C., Pham, A.-T., Meinerzhagen, B., Ringhofer, C., Bollhöfer, M.: Stable discretization of the Boltzmann equation based on spherical harmonics, box integration, and a maximum entropy dissipation principle. J. Appl. Phys. **100**, 024 502-1–024 502-13 (2006)
20. Branin, F.H.: Network sensitivity and noise analysis simplified. IEEE Trans. Circuit Theory **20**, 285–288 (1973)
21. Tsen, K.T., Kiang, J.G., Ferry, D.K., Morkoç, H.: Subpicosecond time-resolved Raman studies of LO phonons in GaN: dependence on photoexcited carrier density. Appl. Phys. Lett. **89**(11), 112111 (2006)
22. Ramonas, M., Matulionis, A., Rota, L.: Monte Carlo simulation of hot-phonon and degeneracy effects in the AlGaN/GaN two-dimensional electron gas channel. Semicond. Sci. Technol. **18**(2), 118 (2003)